Validation of atomic data using a plasma discharge

2010 New J. Phys. 12 073018

(http://iopscience.iop.org/1367-2630/12/7/073018)

New Journal of Physics
The open-access journal for physics

Validation of atomic data using a plasma discharge

Dirk Dodt[1,3], **Andreas Dinklage**[1], **Klaus Bartschat**[2] **and Oleg Zatsarinny**[2]

[1] Max-Planck-Institut für Plasmaphysik, EURATOM Association, Wendelsteinstraße 1, 17491 Greifswald, Germany
[2] Department of Physics and Astronomy, Drake University, Des Moines, IA 50311, USA
E-mail: dirk.dodt@ipp.mpg.de

New Journal of Physics **12** (2010) 073018 (16pp)
Received 26 January 2010
Published 21 July 2010
Online at http://www.njp.org/
doi:10.1088/1367-2630/12/7/073018

Abstract. Using a neon discharge as a well-assessed reference, we demonstrate the validation of atomic data for discharge modeling with data from emission spectroscopy. Specifically, a collisional radiative model of a neon dc discharge was set up using a set of structure and collision data from a semirelativistic *B*-spline *R*-matrix calculation by Zatsarinny and Bartschat (2004 *J. Phys. B: At. Mol. Opt. Phys.* **37** 2173) and the electron-energy distribution function of the plasma was determined from the spectroscopic measurement by Dodt *et al* (2008 *J. Phys. D: Appl. Phys.* **41** 205207). Since the model covers almost the entire visible spectrum, considering a large number of emission lines and many important collisional coupling mechanisms, it enables us to thoroughly test the consistency of the modeled excited-state populations. Inconsistencies, which appear as correction factors for the rate coefficients, are extracted by means of Bayesian probability theory. Despite its limitations, the sensitivity of the approach was sufficient to provide critical information about the collision data, especially in cases where standard cross-section measurements using merged electron and atom beams are difficult to perform. The present approach thus complements existing experimental techniques to test theoretical predictions.

[3] Author to whom any correspondence should be addressed.

Contents

1. Introduction

In a recent paper [1], we described the implementation of a data analysis procedure for the reconstruction of the electron-energy distribution function (EEDF) of a low-temperature plasma from optical emission spectroscopy. The analysis was applied to data from the positive column of a neon direct current (dc) discharge.

The model of the plasma and the spectroscopic measurement employed a complete and internally consistent set of atomic structure and electron collision data generated through semi-relativistic B-spline R-matrix (BSRM) calculations [2], which are essentially a close-coupling ansatz for the solution of the Schrödinger equation of the electron atom system. The probabilistic nature of our approach allowed us to account for possible uncertainties of the atomic dataset as well as other uncertainties of the model, of either experimental or theoretical nature. The consistent propagation of the uncertainties made it possible to state a confidence region of the reconstruction result, which agreed well with published EEDFs from different approaches.

The present follow-up paper focuses on an entirely different aspect of the above work, namely the validation of atomic data using a plasma discharge. The standard way to validate atomic data, both for the target structure (energy and oscillator strengths) and for projectile–target collisions, is a direct comparison of experimental results and theoretical predictions for a given process. For electron–atom collisions, which are of specific interest in the present work, state-selected experiments often involve merged electron and atom beams. As a result, there are numerous challenges that need to be overcome in order to allow for such a comparison [3]. These include, but are not limited to, (i) the preparation of a sufficiently monoenergetic projectile beam, (ii) the preparation of a specific initial target state (usually only the ground state or a metastable excited state is possible owing to the need for a sufficiently long lifetime, unless a suitable laser is available to prepare a mixture of ground and laser-excited states), (iii) the selection of a well-defined final target state (either through light emission in optically allowed transitions or through the energy loss of the projectile) and (iv) the determination of the effective interaction region and the various relevant densities of the

projectile and target beams, as well as the detector efficiencies. As a result, putting experimental cross sections on an absolute scale can be extremely difficult and usually results in significant uncertainties. In fact, often either cross normalization to presumably known other cross sections or assistance from theory is used to put the experimental data on an absolute scale. Of course, this procedure inherits the uncertainties from other measurements and/or theoretical predictions.

In the present paper, we describe a new alternative approach to assess the validity of theoretical predictions. The basic idea is to model a plasma discharge using a large set of atomic data and compare the predicted line radiation of the plasma to measured emission spectra. The probabilistic approach makes it possible to account for an uncertainty in each rate coefficient of the plasma model. If a sufficient number of emission lines is observed, the redundancy in the data allows for a test and the quantification of a refinement of the assumed rate coefficients. The approach is able to identify the coefficients where such a refinement is possible and delivers the uncertainty of the obtained result. A careful assessment of the uncertainties of the plasma model was performed to allow for the correct quantification of the error margins of the refined rate coefficients. A quantitative validation of theoretical models is thus obtained. For some specific cases discussed in this paper, it is even possible to assess the basic physical assumptions entering the numerical calculations.

In the current implementation, however, it is not possible to check the energy dependence of individual cross sections directly. However, we can assess the reliability of the derived rate coefficients, i.e. the cross section convoluted with the EEDF. From an applied point of view, this is the most important test of the theoretical input, since these rate coefficients are required in the modeling of the discharge.

We will demonstrate the potential of the method by investigating electron-impact excitation of neon atoms in the low-energy near-threshold regime. Although the sensitivity is limited, we show that it is indeed possible to confirm many of the input data within the experimental uncertainty and, in some cases, to obtain information about likely problems with these data. Specifically, as discussed below, this is the impact of coupling to high-level Rydberg states as well as the target continuum in electron–atom collisions. It allows one to retrieve experimental evidence regarding the quality of theoretical predictions, for which no direct cross-section measurements or thoroughly assessed theoretical predictions are available in the literature, while plasma modelers are in need of such data.

This paper is structured as follows. Since the details of the atomic data calculations have been published before, we only briefly summarize in section 2 the numerical model used to generate both the target structure and the cross sections for electron impact. In addition, we show an example to demonstrate the need for validation. In section 3, the validation procedure is discussed. This is followed by the presentation of our principal results and their discussion in section 4.

2. Atomic structure and collision models

For the electron impact excitation cross sections and Einstein coefficients, a dataset from semi-relativistic B-spline Breit–Pauli R-matrix (BSRM) calculations was used. Details of these calculations were given by Zatsarinny and Bartschat [2]. Briefly, they are based on a close-coupling description of e–Ne collisions, including the lowest (in energy) 31 *physical* target states. Using term dependent and hence non-orthogonal orbital sets, which were individually optimized for each target state of interest, allowed for a highly accurate target description with a

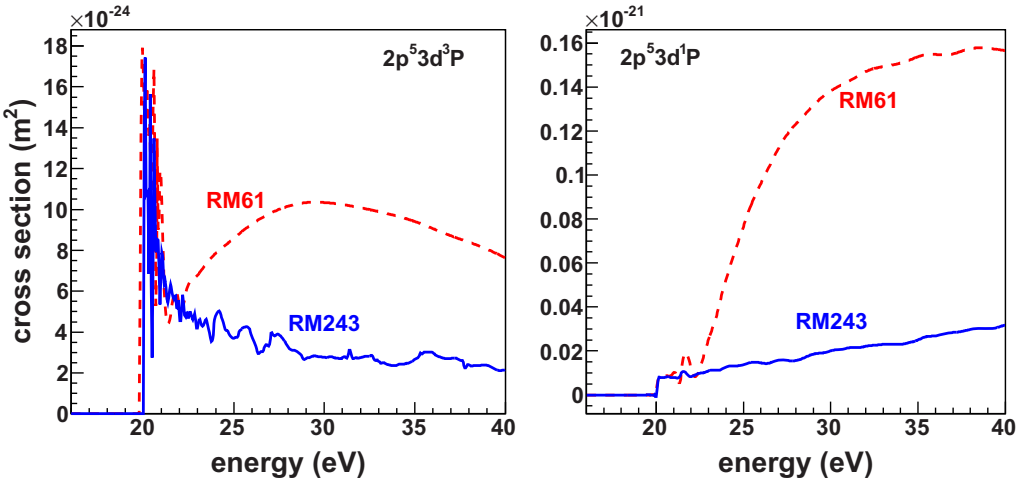

Figure 1. Cross section for electron-impact excitation of the LS-coupled states $(2p^5 3d)^3P$ (left) and $(2p^5 3d)^1P$ (right), as obtained by Ballance and Griffin [5] in non-relativistic R-matrix calculations with 61 and 243 coupled states, respectively (RM61 and RM243). Adapted from [5] with permission from IOP Publishing.

relatively small number of configurations in the configuration-interaction expansion. The above theoretical data were chosen, since they represent a complete, and internally consistent, dataset for all transitions of interest.

Although the above calculation was highly successful in reproducing the metastable excitation function of the $(2p^5 3s)$ states with total electronic angular momenta $J = 0, 2$, as well as the resonance structure near the excitation thresholds of the $(2p^5 3s)$ and $(2p^5 3p)$ states [4], a potential problem with results from such a model was pointed out by Ballance and Griffin [5]. Specifically, they showed that the theoretical predictions for some excitation cross sections are very sensitive to the inclusion of coupling effects to higher Rydberg states, and even more importantly to the target ionization continuum. Especially at the so-called 'intermediate energies', between about one and five times the ionization threshold, accounting for such coupling effects can reduce the results significantly, sometimes by factors of 2–5 rather than just a few per cent. Interestingly, Ballance and Griffin predicted a very strong effect even on the cross sections for the optically allowed transitions from the $(2p^6)^1S_0$ ground state to some of the $(2p^5 3d)$ states with $J = 1$.

Figure 1 shows two examples of their predictions, here for the simplified case of the non-relativistic LS-coupling scheme, which allows for the inclusion of a larger number of 'pseudo-states' (see below) with acceptable computational effort. Although this scheme is inappropriate for the Ne target of interest for the present work, these calculations show that the theoretical cross sections for the $(2p^5 3d)$ states with dominant ^3P and ^1P character change dramatically when coupling to the target continuum is included via a large number of 'pseudo-states', i.e. discrete states of finite range that are obtained by diagonalizing the target Hamiltonian and are used to approximate the coupling to the infinite number of high-lying Rydberg states as well as the ionization continuum.

Unfortunately, the computational resources required for a calculation in the semi-relativistic Breit–Pauli approach made a converged calculation with a sufficiently large number of pseudo-states impossible. Figure 2 exhibits the results for two states of the $2p^5 3d$

Table 1. Dominant mixing coefficients of LS-coupled contributions in the intermediate-coupling description of the three $2p^5 3d$ states in Ne with $J = 1$, as determined in the structure part of the BSR calculation. The squares of these coefficients provide the approximate 'fraction' of the LS character of the respective state. The state label, which is also given, is explained in table 4.

State	Label	^{3}P	^{1}P	^{3}D
$2p^5(^2P^\circ_{3/2})\,3d\,^2[\frac{1}{2}]^\circ$	$3d_{11}$	0.897	0.428	0.108
$2p^5(^2P^\circ_{3/2})\,3d\,^2[\frac{3}{2}]^\circ$	$3d_7$	0.281	0.743	0.607
$2p^5(^2P^\circ_{1/2})\,3d\,^2[\frac{3}{2}]^\circ$	$3d_1$	0.340	0.514	0.787

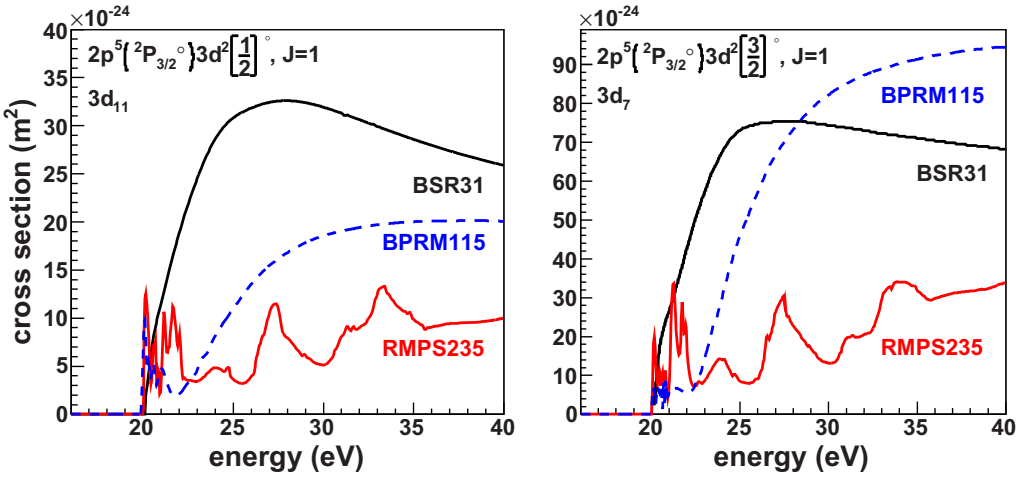

Figure 2. Cross section for electron-impact excitation of the physical states $2p^5(^2P^\circ_{3/2})\,3d\,^2[\frac{1}{2}]^\circ$, $J = 1$ (left) and $2p^5(^2P^\circ_{3/2})\,3d\,^2[\frac{3}{2}]^\circ$, $J = 1$ (right), as obtained by Ballance and Griffin [5] in Breit–Pauli R-matrix calculations with 115 and 235 coupled states (BPRM115 and BSR235), respectively. Also shown are the results from the BSR31 model.

manifold, both with $J = 1$, albeit obtained in non-converged calculations. Once again, we see the dramatic effect of coupling to the continuum, although the structures seen in the theoretical predictions above the ionization threshold are unphysical numerical artifacts due to the discretization procedure with an insufficient number of states. Also shown in this figure are the results from the 31-state BSR model that were used in the modeling of our discharge. For the $2p^5(^2P^\circ_{3/2})\,3d\,^2[\frac{1}{2}]^\circ$, $J = 1$ state, which is predominantly of $^3P_1$ character (see table 1), the BSR31 predictions are generally higher than those from the 61-state Breit–Pauli model (BPRM61) of Ballance and Griffin [5] and show a maximum near 30 eV incident energy, and they lie even further above those from the BPRM235 model that includes a large number of pseudo-states. Similar discrepancies occur for the $2p^5(^2P^\circ_{3/2})\,3d\,^2[\frac{3}{2}]^\circ$, $J = 1$ state, which is predominantly of ^{1}P character. Although not available from the Ballance and Griffin work, the strong mixing of the LS ^{1}P-component in the $2p^5(^2P^\circ_{1/2})\,3d\,^2[\frac{3}{2}]^\circ$, $J = 1$ state (predominantly of ^{3}D character) suggests that the effect on this state may be similar to that on the $2p^5(^2P^\circ_{3/2})\,3d\,^2[\frac{3}{2}]^\circ$, $J = 1$ state.

It is important to recall, however, that the validation procedure described below does not test the cross section directly, but rather the rate coefficient obtained by convoluting the cross section with the EEDF. In our particular case of a low-temperature discharge, this essentially limits the test to the energy range of a few eV above threshold. Looking at figures 1 and 2, therefore, one may reasonably expect that including only physical states in the close-coupling expansion, as done in the BSR31 model, is sufficient for the needs of a discharge modeler. We will see below that this is, indeed, the case for most of the rate coefficients calculated from the BSR31 cross sections in this work. Nevertheless, there are important exceptions. In those cases, the effects of coupling to the continuum, as predicted by Ballance and Griffin [5], are apparently not negligible.

Although we concentrate on the validation of the rate coefficients here, we mention for completeness that data for oscillator strengths from the same BSR model were combined with those from the atomic database of NIST [6]. Where data from NIST are available, a weighted average of the Einstein coefficients was computed using the uncertainties stated by NIST and the ones described below. The cross sections for the ionization of neon in the ground and excited states were taken from [7] and [8].

3. The validation procedure

The rate coefficients of the model for a neon discharge are validated by comparison of the modeled plasma emission to the measured spectra of a discharge. Methods from probability theory are used to assess the significance of discrepancies between the model and measurement, given the precision of the atomic data employed and the experimental uncertainties. Correction factors for the rate coefficients of a collisional radiative model (CRM) of the plasma are inferred using a statistical model of the discharge and the spectroscopic measurement. A Markov-chain Monte-Carlo (MCMC) sampling algorithm is used to find regions in parameter space resulting in a modeled spectrum that is compatible with the measured data *and* the results of the BSRM approach within the specified uncertainties.

From a probability theoretical point of view, the present analysis is an example of a parameter estimation problem in the presence of uncertain information about the model parameters. An introduction to the topic of Bayesian probability theory and its use for problems like the one considered here can be found, for example, in [9]. The methods and software employed for the implementation of the data analysis procedure were developed in the context of the application of Bayesian methods in the magnetically confined fusion community. See [10, 11] and references therein for examples in this context.

In the following, the *forward model* for the spectroscopic measurement will be briefly described. A full description of the model can be found in our previous publication [1]. The relevant uncertainties for the present analysis are discussed and the likelihood and priors (see section 3.3 below) adopted will be described. The concept of marginal distributions, which is used to summarize the results of the analysis, is also briefly introduced.

3.1. Discharge model

The validation of the set of excitation cross sections is based on a model of the plasma discharge and a description of the spectroscopic measurement. Overall, the framework consists of a CRM of the plasma, the integration of the plasma emission over the line of sight of

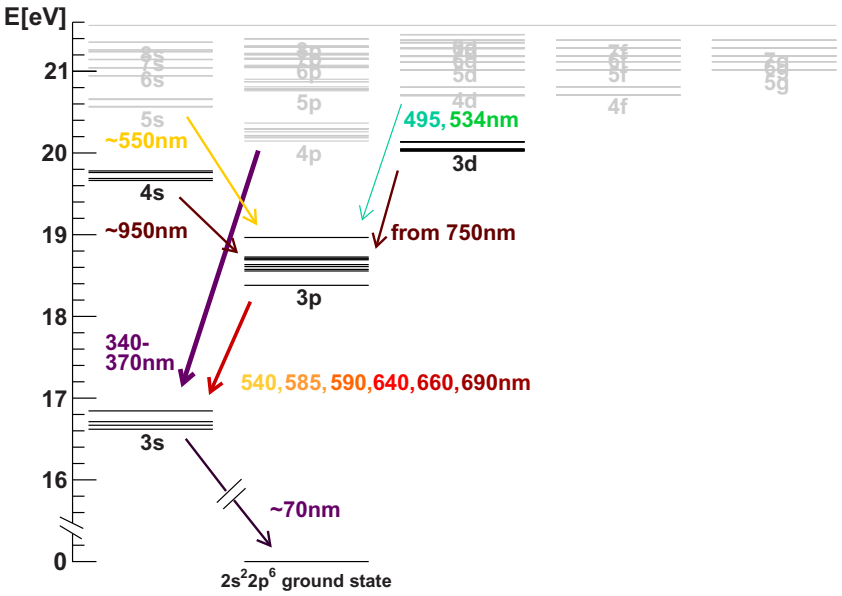

Figure 3. Energy level diagram of neon. The 31 levels incorporated in the CRM are shown in black. The spectral measurement of the plasma emission covers a spectral range of 550–900 nm (see figure 4).

the spectrometer optics, and a description of the spectrometer response (apparatus function, wavelength calibration, calibration of the absolute intensities).

In figure 3, an energy level diagram of neon is shown. In order to model a large fraction of the visible emission spectrum, 31 states are considered in a multiplet resolved CRM. In table 3, a list of the elementary processes considered in the model is given. With respect to the previous publication [1], the CRM was extended by accounting for collisional excitation transfer processes within the 3p multiplet. See also section 3.6 below.

The result of the discharge model is depicted in figure 4 together with the spectral measurement. Good agreement between the model and data over three orders of magnitude of the emitted light intensity can be observed.

In parameter estimation problems, a data model in the form of a set of functions $\vec{D}_{\mathrm{sim}}(\vec{\theta})$ depending on a number of model parameters $\vec{\theta}$, which can be directly compared to the actual measured data $\vec{D}$, is needed. In the present case, the data vector is given by the intensities of the spectrometer pixels at different wavelengths. The most important parameters of the model are the rate coefficients of the CRM and the quantities needed for the description of the spectrometric measurement, such as the parameters of the pixel to wavelength mapping. (See [1] for a complete list of the parameters.)

3.2. Statistical data model

By combining the discharge model with the error statistics of the spectral measurement, a probabilistic model $p(\vec{D}|\vec{\theta}, I)$ for the data is obtained. Here, I abbreviates all information relevant to the inference, such as model assumptions and parameterizations. It is written down explicitly, in order to emphasize the dependence of the assigned probabilities on the validity of the underlying model.

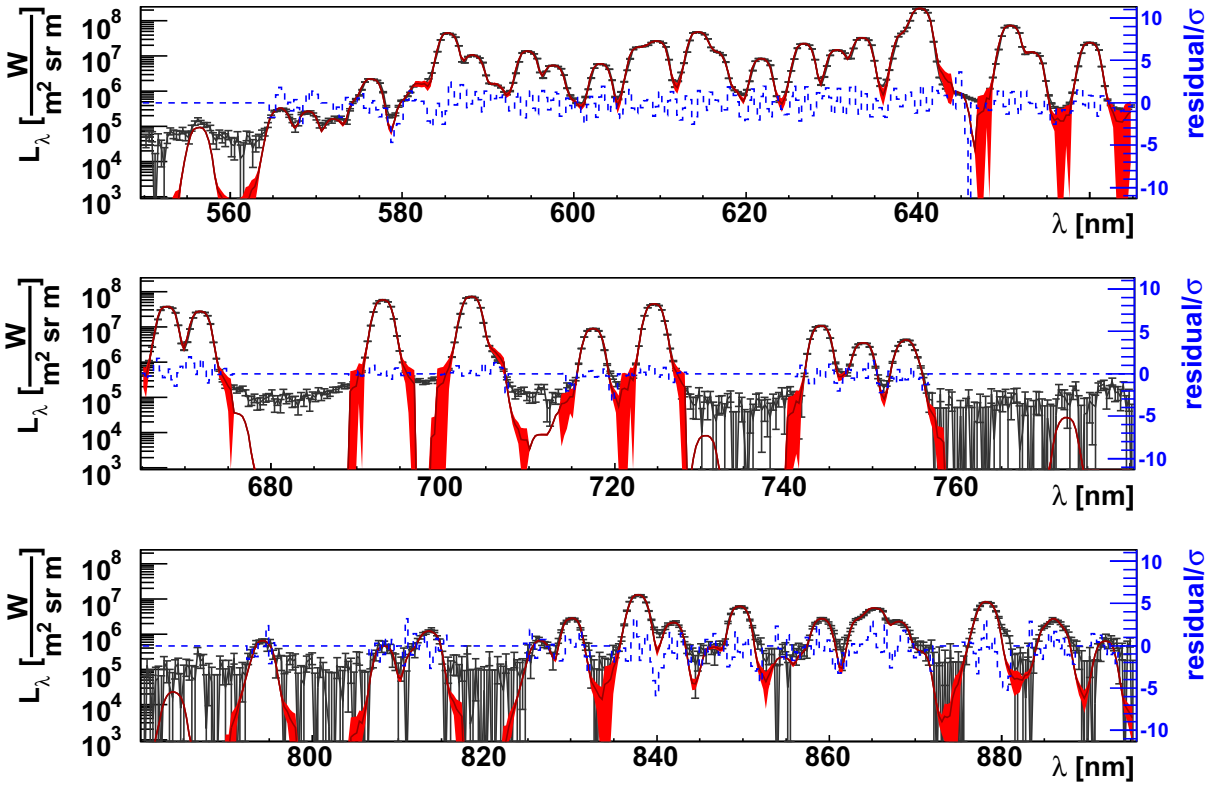

Figure 4. Result of the spectroscopic model of the discharge (red) and the measurement (black). The three rows of the figure show the emission spectrum in the range of 550–900 nm. The logarithmic scale allows us also to depict the lines with low intensity. The red area of the discharge model reflects the uncertainty of the apparatus function, while the black points with error bars show the measured spectrum. The blue dashed curve represents the difference between the model and measurements in units of the standard deviation σ.

The probability density function (PDF) $p(\vec{D}|\vec{\theta},\ I)$ describes the expected distribution of the measured data if $\vec{\theta}$ were the true values of the unknown model parameters. It is called the *likelihood*.

The error statistics of each pixel i of the spectrometer is given by a Gaussian of width σ_i, where σ_i depends on the intensity measured for each pixel (see [1] for more details). Accordingly, the likelihood of the considered spectroscopic data is

$$p(\vec{D}|\vec{\theta},\ I) = C \exp\left\{-\frac{1}{2}\sum_{i=1}^{n}\frac{(D_{\mathrm{sim},i}(\vec{\theta}) - D_i)^2}{\sigma_i^2}\right\}, \tag{1}$$

where n is the number of spectrometer pixels and C is a normalization constant. Since the shape of the PDFs is most relevant for parameter estimations (mainly the location of the maxima and their widths), it is appropriate to discard the normalization. This considerably reduces the computational effort.

3.3. Inference procedure

The starting point for inference about the model parameters $\vec{\theta} = (\theta_1, \theta_2, \ldots)$ is Bayes' theorem. This makes it possible to obtain the PDF $p(\vec{\theta}|\vec{D},\ I)$ from the likelihood through

$$p(\vec{\theta}|\vec{D},\ I) = p(\vec{D}|\vec{\theta},\ I)\frac{p(\vec{\theta}|I)}{p(\vec{D}|I)}. \tag{2}$$

The PDF $p(\vec{\theta}|\vec{D},\ I)$ will be referred to as *posterior* below. It quantifies regimes of the parameter vector that are compatible with a given set of measured data and the additional information quantified by $p(\vec{\theta}|I)$. In the context of parameter estimation from a given measurement $\vec{D}$, $p(\vec{D}|I)$ is a single number that can, in principle, be obtained from the normalization of the posterior. For the purposes of the present paper, however, this calculation can again be omitted.

The PDF $P(\vec{\theta}|I)$ is called *prior*. It quantifies the information available about the model parameters, independent of the considered likelihood. If little is known about a parameter, a 'flat' prior is used, which has non-vanishing values for a broad range of this parameter. For example, this is the case for the parameters of the electron energy distribution of the plasma, which is to be determined by the analysis and not presumed *a priori*. On the contrary, if the value of a parameter is known to a certain precision independent of the currently considered data, as in the case of the correction factors for the rate coefficients in the CRM, the 'informative' prior is a peaked function with significant probability mass only in a well-defined region of parameter space. In [1], a complete list of all model parameters and the chosen priors is given. Flat priors are used for the parameters describing the EEDF of the plasma, as well as for those describing the optical depths of transitions to the metastable states. Gaussian (informative) priors, on the other hand, are used for the parameters associated with the employed atomic data. The width of the respective prior distribution is given by the uncertainty in each parameter, which was estimated as described below.

3.4. Visualization of the validated rate coefficients

The posterior quantifies all the information that can be inferred from the spectroscopic data given the assumptions made in the model. It has the form of a high-dimensional PDF. In order to summarize the obtained corrections for the theoretical rate coefficients in a convenient form, the posterior is projected down to the dimension of a single component θ_i of the parameter vector $\vec{\theta}$ at a time. The function

$$p(\theta_i|\vec{D},\ I) = \int \mathrm{d}\theta_1 \mathrm{d}\theta_2 \ldots \mathrm{d}\theta_{i-1}\mathrm{d}\theta_{i+1} \ldots \mathrm{d}\theta_n\ p(\vec{\theta}|\vec{D},\ I) \tag{3}$$

is called the marginal posterior for θ_i.

3.5. Uncertainty of the employed atomic data

The uncertainty of the employed database of elementary processes is a fundamental ingredient for the validation procedure. This is due to the fact that a correct description of the emission spectrum can only be achieved by adjusting the employed rate coefficients by small amounts compatible with their respective precision.

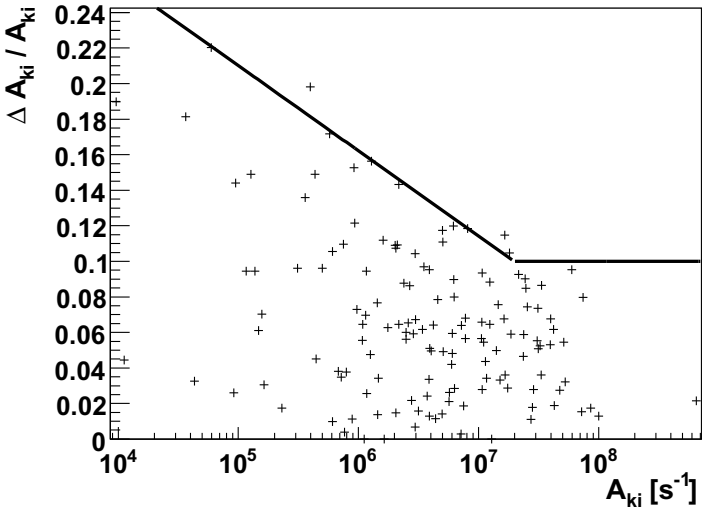

Figure 5. Absolute value of the relative difference $2|A_{ij,(v)} - A_{ij,(l)}|/(A_{ij,(v)} + A_{ij,(l)})$ between the BSRM results for the Einstein coefficients A_{ij} in the length and velocity form of the dipole operator plotted as a function of the absolute value of the Einstein coefficient. The straight line depicts the width (rms) of the prior distribution as a function of the absolute value of the coefficient. See the text for details.

As mentioned above, an unbiased description of the experimental data by the forward model is required for the correct inversion of the model. The probabilistic analysis used here has two desired properties in this context: firstly, the limiting effect of the uncertainty of the plasma model on the precision of the inference about the electron energy distributions is correctly described by the method. The broader the marginalized posterior for the parameters of the EEDF, the more uncertain the atomic data (see also [1]). Secondly, the consideration of the marginalized posteriors for the atomic data themselves potentially allows one to infer additional information about the atomic set. It was ultimately determined (see below) that not all combinations of atomic data, which are compatible with the results from the BSRM calculations within their specified precision, resulted in a correct description of the measured emission spectra.

As stated, the precision of the knowledge about the atomic data needs to be quantified for the validation procedure. This information was determined in the following way:

3.5.1. Uncertainty of the transition probabilities. The results of the structure calculations using the length and the velocity form of the dipole operator were compared. The relative difference between the two, which is an indication of the reliability of the computed Einstein coefficients, is considered as a function of the absolute value of the respective coefficient. The relative width of the prior distribution, as shown in figure 5, is assigned by approximately taking the envelope of the relative difference if it is larger than 10% and 10% otherwise.

3.5.2. Uncertainty of the cross-section scale factors. The uncertainty of the cross-section data was assigned depending on the final state of the transitions. The values were estimated

Table 2. Estimated uncertainties of the excitation cross sections.

Final state	Width of prior distribution (relative error) (%)
$2p^5 3s$, $J = 1$	10
$2p^5 3s$, $J = 2$	20
$2p^5 3p$	40
$2p^5 4s$	60
$2p^5 3d$	60

by comparing the results of different theoretical approaches [4, 5] to the very few available experimental results (see references cited in [4]) and by trying to assess the difficulty of the respective calculations based on past experience. Table 2 lists the estimated uncertainties that were subsequently employed in the model (see table 4 for the labeling of the excited states).

3.6. Robustness of the validation procedure

While the statistically correct description of the measured data by the forward model was directly checked by comparing the measured and simulated data [1] (see also figure 4), the correctness of the physical interpretation of the model parameters, and the robustness against simplifying assumptions, are more difficult to assess. The effect of different model assumptions (radial variation of population densities, flexibility of the parameterization of the EEDF, description of the apparatus function of the spectrometer, optical depth of transitions to metastable excited states) was studied in detail. The results of these considerations are described in the PhD thesis [12].

For the present paper, the CRM was extended further compared to that described in [1] by including rate coefficients for collisional excitation transfer processes within the 3p multiplet. (See table 3 for a full list of all considered elementary processes.) The need for this extension of the model became evident after finding several unexpected deviations in the cross sections for excitations involving the 3p multiplet. It should be noted, however, that the corrections for the transitions to the 3d multiplet (see below), as well as the EEDF reconstruction as discussed in [1], were not significantly affected by this improvement to the model.

The influence of higher-lying atomic states, which are not taken into account by the current CRM, was studied by assuming population densities for all higher states for which radiative transition probabilities are available from the structure calculation [2]. The highest states taken into account in this way are the 9s, 7p, 8d and 7f states. The energy dependence was estimated by fitting the population densities of the atomic states described by the model with an exponentially decreasing function. Rates could thus be obtained and compared to the rates for the excitation processes. It was found that, for states in the 3p multiplet, the population from higher-lying states has a rate of less than 3% of the excitation rate from the ground and 3s states. For states in the 3d multiplet, the contribution would be less than 10% of the excitation from the ground and 3s states (see table 3). Since these corrections are considerably smaller than the uncertainty of the excitation cross sections (see table 2), they were not taken into account.

Table 3. Elementary processes considered in the CRM.

	Elementary process	Treatment in the current model
•	Electron collisions with atoms in the ground and 3s states, exciting the 3s, 3p, 4s and 3d multiplets	BSR31 cross sections
•	Radiative decay of all the considered states	Einstein coefficients from NIST and BSR calculations of the oscillator strengths
•	Electron collisions with atoms in the 3p multiplet and higher states	Neglected
•	Cascade contributions from higher states	Estimated to be less than $\lesssim$3% of the rate of the excitation from the ground and 3s states for the 3p multiplet and $\lesssim$10% for the 3d multiplet
•	Radiation transport	Escape factors from Lawler and Curry [13], effective densities for 3s states [12]
•	Excitation transfer inside 3s and 3p multiplets in Ne+Ne* collisions	Rate coefficients from Steenhuijsen [14] and Paterson *et al* [15]
•	Chemoionization	Rate coefficients from van Schaik *et al* [16]

4. Results and discussion

The inversion of a detailed model of a neon discharge allows for the determination of the EEDF of a low-pressure neon discharge from emission spectroscopic data [1]. In addition, the redundancy caused by the consideration of a large number of observed spectral lines enables the assessment of the consistency of the employed model and hence the validation of the electronic excitation rate coefficients.

The result of the validation procedure is summarized in figure 6, which depicts the marginal distributions of the correction factors for the electronic excitation rate coefficients as obtained by the MCMC procedure. (See table 4 for details of the labels.) We note that the majority of the obtained correction factors show good agreement with a value of 1.0, i.e. showing that a description of the spectroscopic data can be obtained without considerable correction of the atomic input data. Transitions for which no validation is possible, because they do not have a significant impact on the modeled spectra, can be recognized by having obtained marginal distributions that are virtually identical to the prior distributions used. For example, this is the case for a number of transitions shown in the lower right and upper left parts of figure 6, which exhibit very similar distributions. These transitions involve one of the three energetically higher states in the 3s multiplet with a small population density compared to the initial state. For the given discharge parameters (neon pressure 89 Pa, discharge current 15 mA and discharge radius 1.5 cm), they do not contribute much to the population of the observed levels. Hence, no meaningful information about them can be extracted from the spectroscopic data.

Out of the transitions that affect the population of the observed neon levels more strongly, there are two for which particularly significant corrections were obtained. Their values are given in table 5. The final states involved in these transitions contain large mixing coefficients from

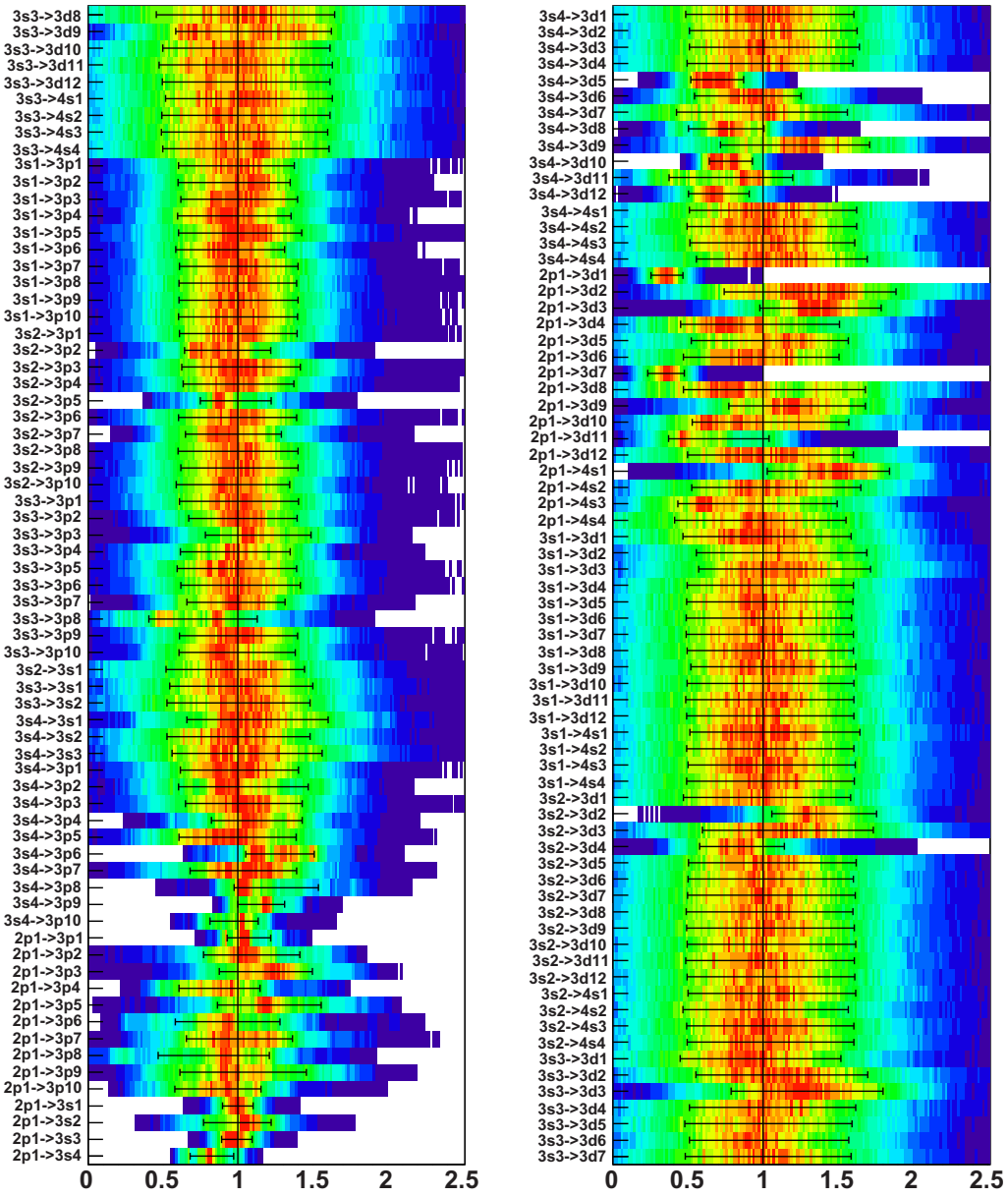

Figure 6. Marginal probability distributions (see section 3.4) for the rate-coefficient correction factors. Each row corresponds to a transition, which is labeled on the left (see table 4). The error bars indicate one standard deviation.

exactly the LS levels, for which Ballance and Griffin [5] found a strong effect of coupling to the continuum (see table 1). According to their calculations, the actual cross sections are indeed expected to be significantly smaller than the original BSRM predictions. This coincides exactly with what we found in our validation procedure.

The results of the (converged) LS-coupling calculations can even be used to estimate the effect of the coupling to the continuum by weighting the respective cross sections with the EEDF and a factor of $\sqrt{2E/m}$. This yields an expected correction factor of $\approx$0.5. Since the properly (i.e. in intermediate coupling) described states have large contributions from different LS states, this can serve as a rough estimate.

Table 4. Short notation of the atomic states used in figure 6.

Label	Configuration in jlK	Energy (eV) (NIST)
$2p_1$	$2p^6\,{}^1S_0$	0
$3s_4$	$2p^5(^2P^\circ_{3/2})\,3s\,^2[\frac{3}{2}]^\circ,\ J=2$	16.619
$3s_3$	$2p^5(^2P^\circ_{3/2})\,3s\,^2[\frac{3}{2}]^\circ,\ J=1$	16.671
$3s_2$	$2p^5(^2P^\circ_{1/2})\,3s\,^2[\frac{1}{2}]^\circ,\ J=0$	16.715
$3s_1$	$2p^5(^2P^\circ_{1/2})\,3s\,^2[\frac{1}{2}]^\circ,\ J=1$	16.848
$3p_{10}$	$2p^5(^2P^\circ_{3/2})\,3p\,^2[\frac{1}{2}],\ J=1$	18.382
$3p_9$	$2p^5(^2P^\circ_{3/2})\,3p\,^2[\frac{5}{2}],\ J=3$	18.555
$3p_8$	$2p^5(^2P^\circ_{3/2})\,3p\,^2[\frac{5}{2}],\ J=2$	18.576
$3p_7$	$2p^5(^2P^\circ_{3/2})\,3p\,^2[\frac{3}{2}],\ J=1$	18.613
$3p_6$	$2p^5(^2P^\circ_{3/2})\,3p\,^2[\frac{3}{2}],\ J=2$	18.637
$3p_5$	$2p^5(^2P^\circ_{1/2})\,3p\,^2[\frac{3}{2}],\ J=1$	18.693
$3p_4$	$2p^5(^2P^\circ_{1/2})\,3p\,^2[\frac{3}{2}],\ J=2$	18.704
$3p_3$	$2p^5(^2P^\circ_{3/2})\,3p\,^2[\frac{5}{2}],\ J=0$	18.711
$3p_2$	$2p^5(^2P^\circ_{1/2})\,3p\,^2[\frac{1}{2}],\ J=1$	18.726
$3p_1$	$2p^5(^2P^\circ_{1/2})\,3p\,^2[\frac{1}{2}],\ J=0$	18.966
$4s_4$	$2p^5(^2P^\circ_{3/2})4s\,^2[\frac{3}{2}]^\circ,\ J=2$	19.664
$4s_3$	$2p^5(^2P^\circ_{3/2})4s\,^2[\frac{3}{2}]^\circ,\ J=1$	19.688
$4s_2$	$2p^5(^2P^\circ_{1/2})4s\,^2[\frac{1}{2}]^\circ,\ J=0$	19.761
$4s_1$	$2p^5(^2P^\circ_{1/2})4s\,^2[\frac{1}{2}]^\circ,\ J=1$	19.780
$3d_{12}$	$2p^5(^2P^\circ_{3/2})\,3d\,^2[\frac{1}{2}]^\circ,\ J=0$	20.025
$3d_{11}$	$2p^5(^2P^\circ_{3/2})\,3d\,^2[\frac{1}{2}]^\circ,\ J=1$	20.026
$3d_{10}$	$2p^5(^2P^\circ_{3/2})\,3d\,^2[\frac{7}{2}]^\circ,\ J=4$	20.035
$3d_9$	$2p^5(^2P^\circ_{3/2})\,3d\,^2[\frac{7}{2}]^\circ,\ J=3$	20.035
$3d_8$	$2p^5(^2P^\circ_{3/2})\,3d\,^2[\frac{3}{2}]^\circ,\ J=2$	20.036
$3d_7$	$2p^5(^2P^\circ_{3/2})\,3d\,^2[\frac{3}{2}]^\circ,\ J=1$	20.040
$3d_6$	$2p^5(^2P^\circ_{3/2})\,3d\,^2[\frac{5}{2}]^\circ,\ J=2$	20.048
$3d_5$	$2p^5(^2P^\circ_{3/2})\,3d\,^2[\frac{5}{2}]^\circ,\ J=3$	20.048
$3d_4$	$2p^5(^2P^\circ_{1/2})\,3d\,^2[\frac{5}{2}]^\circ,\ J=2$	20.136
$3d_3$	$2p^5(^2P^\circ_{1/2})\,3d\,^2[\frac{5}{2}]^\circ,\ J=3$	20.136
$3d_2$	$2p^5(^2P^\circ_{1/2})\,3d\,^2[\frac{3}{2}]^\circ,\ J=2$	20.138
$3d_1$	$2p^5(^2P^\circ_{1/2})\,3d\,^2[\frac{3}{2}]^\circ,\ J=1$	20.140

Table 5. Most significant corrections obtained from the measured spectral data. The initial state of these transitions for which strong corrections were obtained is the ground state.

Initial state	Final state	Configuration	Correction
Ground	$3d_7$	$2p^5(^2P^\circ_{3/2})\,3d\,^2[\frac{3}{2}]^\circ,\ J=1$	$0.36^{+0.12}_{-0.12}$
Ground	$3d_1$	$2p^5(^2P^\circ_{1/2})\,3d\,^2[\frac{3}{2}]^\circ,\ J=1$	$0.35^{+0.11}_{-0.11}$

For the transition from the ground state to the $3d_1$ level, a correction between $0.65^{+0.32}_{-0.29}$, but slightly favoring smaller values (as can be seen by the red area around 0.5 in figure 6 for that transition), is found. This is caused by the fact that for this transition the stepwise excitation via the metastable $3s_4$ state is important. The validation procedure is not able to resolve which of the two excitation channels is overestimated in the atomic dataset, but the sum of both correction factors is determined to be $1.47^{+0.22}_{-0.19}$. This cannot be seen in the simplified visualization using the one-dimensional marginal distribution, but in the two-dimensional marginal posterior of both correction factors. If it is assumed that the cross section for stepwise excitation is correct to a level of 10%, a correction factor of $0.52^{+0.13}_{-0.15}$ for the excitation channel from the ground state is obtained. Again, the $3d_1$ state has a large contribution from the $(2p^5 3d)^1P$ state, for which a strong effect of coupling to the continuum was found by Ballance and Griffin [5].

There are a few other less significant corrections for transitions to the 3d multiplet (see figure 6), which nevertheless suggests that additional information can be inferred from the spectroscopic data. The magnitude of these correction factors is compatible with the assumed precision of the theoretical cross sections. The direction of the obtained correction factor (smaller or greater than unity) can serve as an indication of the reliability of the predicted cross section near the excitation threshold.

5. Summary

We have presented a method to validate atomic input data by comparing predictions from a detailed CRM of a neon discharge with the direct measurement of the optical emission spectrum. Specifically, we tested the suitability of oscillator strengths and cross sections for electron collisions obtained in a recent semi-relativistic BSRM calculation for modeling the discharge. In the vast majority of cases, we found that the atomic input data, and our CRM, were sufficiently accurate to reproduce the measured spectrum. This result is an important validation of the basic atomic data.

Moreover, we detected a few significant exceptions that qualitatively confirmed an independent theoretical prediction about the importance of accounting for coupling to the target continuum in the numerical treatment of e–Ne collisions. This result is important for (i) atomic physicists as the data producers, giving experimental evidence for the need to include pseudo-states in their models, and (ii) the plasma modeling community as users of these data, which had not been validated by either beam experiments for state-to-state transitions or theoretical predictions from a presumably converged calculation.

The present results are, to our knowledge, the first experimental evidence supporting theoretical considerations regarding the impact of high-level Rydberg states and continuum coupling on the results for electron collisions from the complex neon target. It is remarkable that they could be obtained using a relatively simple experiment like a dc glow discharge.

Acknowledgments

KB and OZ were supported by the United States National Science Foundation under grants PHY-0757755 and PHY-0903818. The authors are indebted to Rainer Fischer for valuable discussions.

References

[1] Dodt D, Dinklage A, Fischer R, Bartschat K, Zatsarinny O and Loffhagen D 2008 *J. Phys. D: Appl. Phys.* **41** 205207

[2] Zatsarinny O and Bartschat K 2004 *J. Phys. B: At. Mol. Opt. Phys.* **37** 2173

[3] Bartschat K, Burke P G and Crowe A 2009 Electron scattering by atoms, ions, and molecules *Encyclopedia of Applied Spectroscopy* ed D L Andrews (Weinheim: Wiley-VCH) p 209

[4] Allan M, Franz K, Hotop H, Zatsarinny O and Bartschat K 2006 *J. Phys. B: At. Mol. Opt. Phys.* **39** L139

[5] Ballance C and Griffin D 2004 *J. Phys. B: At. Mol. Opt. Phys.* **37** 2943

[6] Ralchenko Y, Jou F-C, Kelleher D E, Kramida A E, Musgrove A, Reader J, Wiese W L and Olsen K 2007 *NIST Atomic Spectra Database* (version 3.1.3) (Gaithersburg: National Institute of Standards and Technology) http://physics.nist.gov/asd3

[7] Wetzel R, Baiocchi F, Hayes T and Freund R 1987 *Phys. Rev.* A **35** 559

[8] Vriens L and Smeets A H M 1980 *Phys. Rev.* A **22** 940

[9] Sivia D and Skilling J 2006 *Data Analysis: A Bayesian Tutorial* 2nd edn (Oxford: Oxford University Press)

[10] Dinklage A, Fischer R and Svensson J 2004 *Fusion Sci. Technol.* **46** 355

[11] Fischer R and Dinklage A 2004 *Rev. Sci. Instrum.* **75** 4237

[12] Dodt D 2009 Determination of the electron energy distribution function of a low temperature plasma from optical emission spectroscopy *PhD Thesis* University of Greifswald, Germany, online at http://ub-ed.ub.uni-greifswald.de/opus/volltexte/2009/649/

[13] Lawler J E and Curry J J 1998 *J. Phys. D: Appl. Phys.* **31** 3235

[14] Steenhuijsen L W G 1981 *Beiträge aus der Plasmaphysik* **21** 301

[15] Paterson A M, Smith D J, Borthwick I S and Stewart R S 2001 *J. Phys. B: At. Mol. Opt. Phys.* **34** 1815

[16] van Schaik N, Steenhuijsen L W G, van Bommel P J M and Verspaget F H P 1979 *J. Phys. Colloq.* **40** C7–97